Control and Cybernetics

vol. **43** (2014) No. 2

Adaptive finite elements based on sensitivities for topological mesh changes

by

Jan Friederich[1], Günter Leugering[2], and Paul Steinmann[1]

[1]Chair of Applied Mechanics, Friedrich-Alexander University Erlangen, Egerlandstr. 5, 91058 Erlangen, Germany
[2]Chair of Applied Mathematics 2, Friedrich-Alexander University Erlangen, Cauerstr. 11, 91058 Erlangen, Germany
jan.friederich@ltm.uni-erlangen.de, leugering@math.fau.de, paul.steinmann@ltm.uni-erlangen.de

Abstract: We propose a novel approach to adaptive refinement in FEM based on local sensitivities for node insertion. To this end, we consider refinement as a continuous graph operation, for instance by splitting nodes along edges. Thereby, we introduce the concept of the topological mesh derivative for a given objective function. For its calculation, we rely on the first-order asymptotic expansion of the Galerkin solution of a symmetric linear second-order elliptic PDE. In this work, we apply this concept to the total potential energy, which is related to the approximation error in the energy norm. In fact, our approach yields local sensitivities for minimization of the energy error by refinement. Moreover, we prove that our indicator is equivalent to the classical explicit a posteriori error estimator in a certain sense. Numerical results suggest that our method leads to efficient and competitive adaptive refinement.

Keywords: adaptive mesh refinement, sensitivity-based refinement, topological sensitivity, asymptotic expansion

1. Introduction

In the last decades, error estimation and adaptivity in the finite element method (FEM) have evolved to an indispensable tool for the numerical solution of partial differential equations (PDEs) in science and engineering. Starting with a rather coarse discretization, the goal of adaptivity is to reduce the approximation error of the discrete solution to the unknown true solution with minimal cost by local refinement. To this end, adaptive algorithms typically rely on local error estimators or indicators that can be computed from given data and a previous discrete solution. There is a number of efficient a posteriori error estimation techniques available, which are, for instance, based on explicit estimation of the

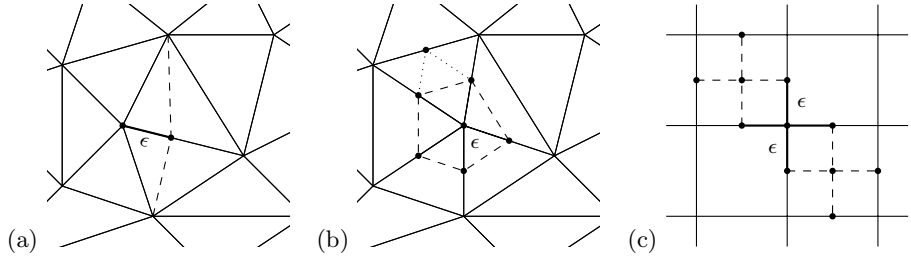

Figure 1. Continuous graph operations on finite element meshes: (a) Insertion of one node along an edge, leading to the subdivision of the adjacent triangles. (b) Insertion of nodes along the edges of a star-shaped subgraph; the appearance of non-simplicial elements can be resolved by the introduction of hanging nodes or bisection of the quadrilaterals. (c) Insertion of nodes in a structured mesh of rectangular elements

residual, solution of local subproblems, hierarchical bases, recovery of the gradient, and several more. For a comprehensive overview of established methods, we refer to Verfürth (1996) or Ainsworth and Oden (2000). Instead of reducing the global error, one might also be interested in the approximation error with respect to a certain output functional, such as point values or boundary fluxes, which leads to the notion of goal-oriented error estimation and refinement, see for instance Bangerth and Rannacher (2003). The literature on applications of these concepts in engineering is vast, see e.g. Stein (2003) for problems in solid mechanics.

In this work, we propose a novel approach to adaptive refinement by calculating *sensitivities* for a given objective function with respect to topological changes of the underlying finite element mesh. To this end, we think of the insertion of new nodes (and hence edges and elements) as a continuous operation on the edge graph of the triangulation, for instance by splitting nodes along edges. Some possible scenarios for node insertion are depicted in Fig. 1 for triangular and quadrilateral meshes in two space dimensions, where the continuous change is parametrized in the variable $\epsilon > 0$. This approach allows for the definition of a topological mesh derivative DJ for a given objective functional J: if u_h and u_h^ϵ are finite element solutions on the current mesh $\mathcal{T}_h$ and the refined mesh $\mathcal{T}_h^\epsilon$, respectively, we define

$$DJ(u_h) := \lim_{\epsilon \to 0} \frac{J(u_h^\epsilon) - J(u_h)}{\epsilon}.$$

These sensitivities can, in turn, be used to introduce local indicators for adaptive refinement.

As a basic application of our approach as well as a proof of concept, we consider in this work the total potential energy J_e of a linear symmetric second-order elliptic PDE. Recalling the well-known relation between J_e and the error

$|||u_h - u|||$ in the energy norm,

$$|||u_h^\epsilon - u|||^2 - |||u_h - u|||^2 = 2\left(J_e(u_h^\epsilon) - J_e(u_h)\right),$$

the topological mesh derivative $DJ_e(u_h)$ yields edge-wise sensitivities for minimization of the energy error. Hence, in contrast to standard adaptive finite element methods, which typically rely on a posteriori error estimators, our approach to adaptivity follows the concept of sensitivity-based mesh optimization by local refinement.

Although our indicators result from a completely different concept, we will prove equivalence to the explicit residual-based error estimator, rendering our method efficient for adaptive refinement. Likewise, this result confirms the effectivity of classical error estimators as local refinement indicators from an optimization point of view. However, we stress that our indicator is – by construction – not an error estimator, as it is based on the first-order approximation to the decrease of the error upon refinement rather than the current local error itself. Consequently, an accurate relation of the sum of local sensitivities to the current global error is not to be expected, and our method seems not to be suited for error estimation and error control. On the other hand, in comparison to the explicit residual-based error estimator in an adaptive algorithm, the relation between indicator value and *error reduction* upon refinement seems to be more accurately captured. This property is of particular importance in cases where possibly large local errors are (almost) orthogonal to the proposed refinements.

In that, our results for minimization of the energy error are rather related to the so-called correction indicators introduced by Zienkiewicz et al. (1983), see also Zienkiewicz and Craig (1986). There, the original motivation had been to predict the decrease of the (quadratic) error upon adding a new degree of freedom in a hierarchical bases setting. Eventually, these ideas led to the development of hierarchical bases estimators (Bank and Smith, 1993; Bank, 1996; Deuflhard et al., 1989). Other than that – except for the rediscovery by Aguilar and Goodman (2006) in the context of anisotropic refinement – the original concept of correction indicators has not been pursued further to the knowledge of the authors. Anyway, since our approach also builds on the insertion of a new basis function, the sensitivities for the total potential energy derived in this paper appear to be similar to the correction indicators from Zienkiewicz et al. (1983) and Aguilar and Goodman (2006) in both structure and performance. However, our concept and its presentation will be more general, as it is not confined to the special application to energy error minimization, but can, in particular, also be employed for various objective functions J. These applications will be studied more extensively in a forthcoming publication.

On the one hand, our idea is motivated by the work of Delfour et al. (1985), where the total potential energy has been employed as the objective function in the context of r-adaptive mesh optimization. There, the corresponding sensitivities for re-localization of nodes have been derived by means of the speed method known from shape optimization (Sokolowski and Zolésio, 1992). Hence, in view

of the recent development towards topological sensitivity analysis (Sokolowski and Zochowski, 1999), our concept extends the approach of Delfour et al. (1985) to topological mesh changes. However, instead of adopting the abstract connection of shape and topological derivatives as in Novotny et al. (2003), we will calculate the asymptotic expansions for topological mesh changes directly without relying on the results of Delfour et al. (1985).

Furthermore, our work is inspired by the ideas of Leugering and Sokolowski (2008, 2011), where the authors derive sensitivities for topological changes on graphs that are governed by partial differential equations, such as networks of beams or strings. Although our problem might look somewhat similar at the first sight, from a conceptual point of view, insofar as we consider topological changes of the edge *graph* of the finite element discretization, our problem differs in some fundamental respects: in our case, functions are defined on elements, that will collapse to edges or nodes in the limit. Secondly, since we are concerned with the asymptotic analysis of a discretized PDE, our problem is in essence finite-dimensional. Nevertheless, some ideas, as well as the overall intuition, are related to Leugering and Sokolowski (2008, 2011).

In this contribution, we will restrict ourselves to the model problem of a linear symmetric second-order elliptic PDE and piecewise linear FEM. Comments on possible extensions will be given throughout this work. Earlier, we have considered our approach in the context of a one-dimensional model problem, see Friederich et al. (2012). In the present work, those results are extended to two and three dimensions and are therefore included as a special case.

This paper is organized as follows: In Section 2, we introduce the model problem and the refinement operation that we consider along with all relevant notation. In Section 3, we derive the asymptotic expansions of finite element solutions with respect to node insertion and obtain the notion of the topological mesh derivative for general objective functions. In Section 4, we apply our results to the total potential energy and define refinement indicators for minimization of the energy error; further, we prove its relation to the residual-based error estimator. Section 5 is devoted to the examination of the performance and reliability of our indicator on the basis of some numerical experiments. We conclude this paper with some comments on goal-oriented refinement in Section 6.

2. Preliminaries

2.1. Model problem

We consider a symmetric linear second-order elliptic PDE on a polygonal Lipschitz domain $\Omega \in \mathbb{R}^d$, $d = 2, 3$, with homogeneous Dirichlet boundary data and an arbitrary right hand side $f \in L^2(\Omega)$, given in weak form as

$$(P)\begin{cases}\text{Find } u \in V := H_0^1(\Omega) \text{ s.th.}\\ a_\Omega(u,v) = (f,v)_\Omega \quad \forall\, v \in V,\end{cases}$$

where

$$a_\Omega(u,v) := \int_\Omega \boldsymbol{K}(x)\nabla u \cdot \nabla v + c(x)\, u\, v \,\mathrm{d}x,$$
$$(f,v)_\Omega := \int_\Omega f\, v \,\mathrm{d}x.$$

For the coefficients we require that $\boldsymbol{K} \in L^\infty(\Omega)^{d\times d}$ be symmetric and uniformly positive definite, and $c \in L^\infty(\Omega)$ non-negative, such that problem (P) admits a unique solution. In addition, we assume that $\boldsymbol{K}$ and c are at least continuous on every element of a given simplicial conformal triangulation $\mathcal{T}_h$. For the main result of Section 4, we will confine ourselves further to piecewise constant coefficients $\boldsymbol{K}$. Considering the ansatz space

$$V_h := \left\{ v_h \in V \cap C(\overline{\Omega}) : v_h|_T \in \mathcal{P}_1(T)\ \forall\, T \in \mathcal{T}_h \right\}$$

of element-wise linear polynomials, the Galerkin approximation of (P) in V_h reads then

$$(P_h)\ \begin{cases} \text{Find } u_h \in V_h \text{ s.th.} \\ a_\Omega(u_h, v_h) = (f, v_h)_\Omega \quad \forall\, v_h \in V_h. \end{cases}$$

Remark 1 *The restriction to symmetric equations and homogeneous Dirichlet boundary data is for the ease of presentation. Our results on the asymptotic expansions for element insertion in Section 3 can be easily generalized to non-symmetric equations with non-homogeneous Dirichlet or Neumann boundary data. However, the extension to higher-order elements is a different scenario, as it requires a greater amount of notational and technical effort.*

Furthermore, we denote the sets of nodes and edges of the triangulation $\mathcal{T}_h$ by $\mathcal{N}_h$ and $\mathcal{E}_h$, respectively, and define the subsets of interior nodes $\mathcal{N}_h^\Omega = \{\boldsymbol{x} \in \mathcal{N}_h : \boldsymbol{x} \notin \partial\Omega\}$ and interior edges $\mathcal{E}_h^\Omega = \{E \in \mathcal{E}_h : E \cap \Omega \neq \emptyset\}$. We let φ_i be the linear Langrangian basis function, associated with any node $\boldsymbol{x}_i \in \mathcal{N}_h$, where we assume for ease of notation that the nodes are numbered so that $\mathcal{N}_h^\Omega = \{\boldsymbol{x}_i\}_{i=1}^N$ and consequently

$$V_h = \mathrm{lin}(\{\varphi_i\}_{i=1}^N), \qquad N = \dim V_h.$$

Moreover, the L^2-norm and the energy norm will be denoted by

$$\|\,.\,\|_\Omega := (\,.\,,\,.\,)_\Omega^{1/2},$$
$$|||\,.\,|||_\Omega := a_\Omega(\,.\,,\,.\,)^{1/2},$$

respectively. Note that $|||\,.\,|||_\Omega$ is equivalent to the usual norm $\|\,.\,\|_V := (\|\,.\,\|_\Omega^2 + \|\nabla\,.\,\|_\Omega^2)^{1/2}$ on $V = H_0^1(\Omega)$. Furthermore, we will make use of the notation $\langle\,.\,,\,.\,\rangle_W : W' \times W \to \mathbb{R}$ for the dual pairing on any space W.

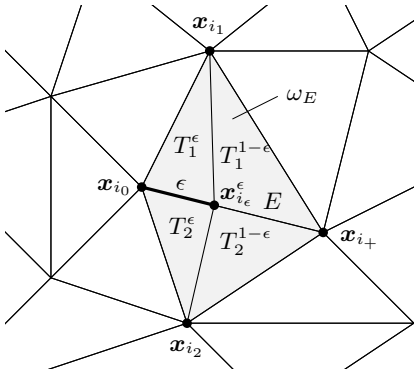

Figure 2. Insertion of node $\boldsymbol{x}_{i_\epsilon}^\epsilon$ along edge $E = (\boldsymbol{x}_{i_0}, \boldsymbol{x}_{i_+})$. The adjacent elements $T_j \subset \omega_E$ are split into pairs $\{T_j^\epsilon, T_j^{1-\epsilon}\}$, $j = 1, 2$

2.2. Insertion of a node along an edge

In this work, we consider the simplest mesh change possible as depicted in Fig. 1 a). Here, only one additional node is inserted and depends on $\epsilon > 0$. Let us introduce the relevant notation for this process in the following: We consider two arbitrary neighboring nodes $\boldsymbol{x}_{i_0}, \boldsymbol{x}_{i_+} \in \mathcal{N}_h$, which are connected by an interior edge

$$E := (\boldsymbol{x}_{i_0}, \boldsymbol{x}_{i_+}) = \operatorname{conv}\{\boldsymbol{x}_{i_0}, \boldsymbol{x}_{i_+}\} \in \mathcal{E}_h^\Omega.$$

More precisely, we assume that at least $\boldsymbol{x}_{i_0} \in \mathcal{N}_h^\Omega$ or $\boldsymbol{x}_{i_+} \in \mathcal{N}_h^\Omega$. We denote the immediate neighborhood of elements sharing edge E by

$$\omega_E := \bigcup_{\substack{E \subset \partial T \\ T \in \mathcal{T}_h}} T.$$

Now, we split node $\boldsymbol{x}_{i_0}$ along the edge $E = (\boldsymbol{x}_{i_0}, \boldsymbol{x}_{i_+})$ as depicted in Fig. 2: For given $\epsilon > 0$ we insert the additional node

$$\boldsymbol{x}_{i_\epsilon}^\epsilon := \boldsymbol{x}_{i_0} + \epsilon(\boldsymbol{x}_{i_+} - \boldsymbol{x}_{i_0}) \in E,$$

and divide each adjacent element $T_j \subset \omega_E$ into pairs $T_j = T_j^\epsilon \cup T_j^{1-\epsilon}$ by new edges (or faces, respectively) for $j = 1, \ldots, M_E$, where M_E is the number of neighboring elements in ω_E. Note that we have $M_E = 2$ if $d = 2$ and $M_E \geq 3$ if $d = 3$. We abbreviate for later use

$$\omega_E^\epsilon := \bigcup_{1 \leq j \leq M_E} T_j^\epsilon, \qquad \omega_E^{1-\epsilon} := \bigcup_{1 \leq j \leq M_E} T_j^{1-\epsilon}.$$

The insertion of the new node along with subdivision of neighboring elements leads to the *refined* triangulation

$$\mathcal{T}_h^\epsilon := (\mathcal{T}_h \setminus \{T_j\}_{j=1}^{M_E}) \cup \{T_j^\epsilon, T_j^{1-\epsilon}\}_{j=1}^{M_E}.$$

Defining the ansatz space of piecewise linear elements on $\mathcal{T}_h^\epsilon$ accordingly,

$$V_h^\epsilon := \{v_h^\epsilon \in V : v_h^\epsilon|_T \in \mathcal{P}_1(T) \,\forall\, T \in \mathcal{T}_h^\epsilon\},$$

we consider the corresponding Galerkin problem

$$(P_h^\epsilon) \begin{cases} \text{Find } u_h^\epsilon \in V_h^\epsilon \text{ s.th.} \\ a_\Omega(u_h^\epsilon, v_h^\epsilon) = (f, v_h^\epsilon)_\Omega \quad \forall\, v_h^\epsilon \in V_h^\epsilon. \end{cases}$$

REMARK 2 *Note that the family of refined triangulations $\{\mathcal{T}_h^\epsilon\}_{\epsilon>0}$ fails to be shape regular as $\epsilon \to 0$. This being a disaster from the numerical point of view for infinitesimally small $\epsilon > 0$, let us remind the reader that we are only interested in the analytical derivation of asymptotic expansions, whereas any mesh modification based on the resulting criteria will be finite, e.g. corresponding to $\epsilon = \frac{1}{2}$. Let us also remark that the usual a priori error estimates continue to hold in this situation, as the maximum angle within the triangulations $\{\mathcal{T}_h^\epsilon\}_{\epsilon>0}$ stays bounded independently of $\epsilon > 0$ (see Babuška and Aziz, 1976).*

Further, we observe that $V_h \subset V_h^\epsilon \subset V$, and more precisely

$$V_h^\epsilon = V_h \oplus \operatorname{lin}\{\varphi_{i_\epsilon}^\epsilon\} = \operatorname{lin}(\{\varphi_i\}_{i=1}^N \cup \{\varphi_{i_\epsilon}^\epsilon\}).$$

Here, $\{\varphi_i\}_{i=1}^N \subset V_h$ are the Lagrangian nodal basis functions of V_h, corresponding to the (interior) nodes $\{\boldsymbol{x}_i\}_{i=1}^N$, and $\varphi_{i_\epsilon}^\epsilon \in V_h^\epsilon$ is the piecewise linear shape function corresponding to the inserted node $\boldsymbol{x}_{i_\epsilon}^\epsilon$, defined by $\varphi_{i_\epsilon}^\epsilon(\boldsymbol{x}_{i_\epsilon}^\epsilon) = 1$ and $\varphi_{i_\epsilon}^\epsilon(\boldsymbol{x}_j) = 0$ for all $\boldsymbol{x}_j \in \mathcal{N}_h$. The situation is depicted in Fig. 3 for $d = 1$. In this context, we also observe that $\varphi_{i_\epsilon}^\epsilon$ converges to a discontinuous function,

$$\varphi_{i_\epsilon}^\epsilon \to \varphi_{i_0}\chi_{\omega_E} \begin{cases} \text{in } L^p(\Omega), 1 \le p < \infty, \\ \text{weakly-}* \text{ in } BV(\Omega), \end{cases} \tag{1}$$

as $\epsilon \to 0$, where χ_{ω_E} denotes the characteristic function of ω_E. For the definition and properties of weak-$*$ convergence in $BV(\Omega)$, we refer to Ambrosio et al. (2000).

For later use, let us also introduce the reference elements $\hat{T}_j = \hat{T}_j^\epsilon \cup \hat{T}_j^{1-\epsilon}$ and affine mappings $\hat{\boldsymbol{F}}_{T_j} : \hat{T}_j \to T_j$ for $j = 1, \ldots, M_E$, as depicted in Fig. 4 for the case of $d = 2$. Moreover, we define the modified coefficient function $\boldsymbol{K}_{i_0,i_+}$ through the identity

$$\boldsymbol{K}_{i_0,i_+} \circ \hat{\boldsymbol{F}}_j(\hat{x}_1, \hat{x}_2) = \lim_{\hat{\xi}\to 0} \boldsymbol{K} \circ \hat{\boldsymbol{F}}_j(\hat{\xi}, \hat{x}_2) \quad \forall (\hat{x}_1, \hat{x}_2) \in \hat{T}_j, \quad j = 1, \ldots, M_E. \tag{2}$$

In other words, *boldsymbol*K_{i_o,i_+} extends the values of $\boldsymbol{K}$ from the edges (faces) containing $\boldsymbol{x}_{i-0}$ onto ω_E on level lines that are parallel to E. In particular, note that $\boldsymbol{K}_{i_0,i_+} \equiv \boldsymbol{K}$ if $\boldsymbol{K}$ is element-wise constant.

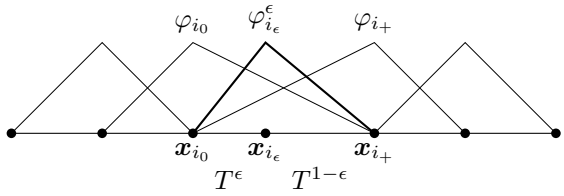

Figure 3. Basis functions $(\{\varphi_i\}_{i=1}^N \cup \{\varphi^\epsilon_{i_\epsilon}\}) \subset V_h^\epsilon$ in $d = 1$. The canonical basis of $V_h = \mathrm{lin}\{\varphi_i\}_{i=1}^N$ is supplemented by the new shape function $\varphi^\epsilon_{i_\epsilon}$ such that $V_h^\epsilon = \mathrm{lin}(\{\varphi_i\}_{i=1}^N \cup \{\varphi^\epsilon_{i_\epsilon}\})$. See also Krysl et al. (2003)

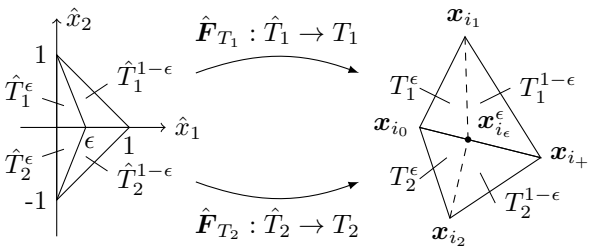

Figure 4. Reference elements $\hat{T}_j = \hat{T}_j^\epsilon \cup \hat{T}_j^{1-\epsilon}$ and affine mappings $\hat{\boldsymbol{F}}_{T_j} : \hat{T}_j \to T_j$, $j = 1, 2$

2.3. Definition of the topological mesh derivative

We are now in the position to define the sensitivity of a given functional $J : V \to \mathbb{R}$ with respect to insertion of a new node along an edge as follows:

Definition 1 *The* topological mesh derivative *of J with respect to insertion of a new node at $\boldsymbol{x}_{i_0}$ along edge $E = (\boldsymbol{x}_{i_0}, \boldsymbol{x}_{i_+})$ is – if it exists – defined as*

$$D_{i_0,i_+} J(u_h) := \lim_{\epsilon \to 0} \frac{J(u_h^\epsilon) - J(u_h)}{\epsilon}. \tag{3}$$

Let us point out that the existence of the topological mesh derivative can indeed not be granted for arbitrary $J : V \to \mathbb{R}$. This issue will be clarified in the course of this paper. Nevertheless, although additional assumptions and special treatment might be needed in some cases, our concept seems to be suitable for many applications of practical interest, see the discussion in Remark 4 below.

3. Asymptotic analysis for finite element solutions

Our results rely on the first-order asymptotic expansion of u_h^ϵ for $\epsilon > 0$, which shall be derived in the following. Standard notation and results from functional

analysis (see, for instance, Reddy, 1998; Alt, 2002) will be used without further reference.

3.1. Continuity for $\epsilon \to 0$

First, we are going to prove that solutions u_h^ϵ of (P_h^ϵ) converge indeed to the solution u_h of (P_h) as $\epsilon \to 0$. To this end, let us first prove the following preliminary result:

LEMMA 1 *It holds that $V_h^\epsilon \to V_h$ in V in the sense of Kuratowski-Mosco, in particular:*

a) Let $\{v_h^\epsilon\}_{\epsilon>0} \subset V$, $v_h^\epsilon \in V_h^\epsilon$, s.th. $v_h^\epsilon \rightharpoonup v$ in V as $\epsilon \to 0$. Then $v \in V_h$.

b) For any $v_h \in V_h$, there exists $\{v_h^\epsilon\}_{\epsilon>0} \subset V$, $v_h^\epsilon \in V_h^\epsilon$, s.th. $v_h^\epsilon \to v_h$ in V.

Proof To prove the first statement, define for $\delta > 0$ the space of functions of V which are piecewise linear on $\Omega \setminus \omega_E^\delta$,

$$W_h^\delta := \left\{ v \in V : v|_T \in \mathcal{P}_1(T) \; \forall\, T \in \mathcal{T}_h^\delta \setminus \{T_j^\delta\}_{j=1}^{M_E} \right\}.$$

It is easy to see that $V_h^\epsilon \subseteq W_h^\delta$ for all $\epsilon \leq \delta$ and that W_h^δ is a closed linear subspace of V, such that $v_h^\epsilon \rightharpoonup v \in W_h^\delta$ weakly in V for any $\delta > 0$. Thus,

$$v \in \bigcap_{\delta>0} W_h^\delta = \{ w \in V : w|_T \in \mathcal{P}_1(T) \; \forall\, T \in \mathcal{T}_h \} = V_h.$$

Note, in particular, that $v \in C(\overline{\Omega})$ is automatically satisfied, see Ciarlet (2002, Thm. 4.2.1). The second assertion is obvious since $V_h \subset V_h^\epsilon$. □

Using this basic observation, continuity of solutions u_h^ϵ in V for $\epsilon \to 0$ is an immediate consequence of the a priori stability estimate:

LEMMA 2 *Let u_h^ϵ and u_h be the solutions of (P_h^ϵ) and (P_h), respectively. Then we have $u_h^\epsilon \to u_h$ in V as $\epsilon \to 0$.*

Proof Due to the coercivity of $a_\Omega(.,.)$ and the continuity of $(f,.)_\Omega$ we may estimate

$$c_a \, \|u_h^\epsilon\|_V^2 \leq a_\Omega(u_h^\epsilon, u_h^\epsilon) = (f, u_h^\epsilon)_\Omega \leq \|f\|_{V'} \|u_h^\epsilon\|_V$$

with the coercivity constant $c_a > 0$, and hence arrive at the classical stability estimate

$$\|u_h^\epsilon\|_V \leq C,$$

which holds independently of $\epsilon > 0$. Therefore, we deduce the existence of a subsequence $\{u_h^\epsilon\}_{\epsilon>0} \subset V$, also denoted by ϵ, such that $u_h^\epsilon \rightharpoonup w$ weakly in V as $\epsilon \to 0$. In the limit, we have

$$a_\Omega(w, v_h) = (f, v_h)_\Omega \quad \forall\, v_h \in V_h \tag{4}$$

and may therefore conclude that the whole sequence converges to w as $\epsilon \to 0$. Furthermore, because $w \in V_h$, due to Lemma 1, we finally identify $w = u_h$ as the unique solution of (4). To prove strong convergence in V, we may equip V with the equivalent energy norm $|||\,.\,|||_\Omega$ and observe that

$$|||u_h^\epsilon|||_\Omega^2 = a_\Omega(u_h^\epsilon, u_h^\epsilon) = (f, u_h^\epsilon)_\Omega \xrightarrow{\epsilon \to 0} (f, u_h)_\Omega = a_\Omega(u_h, u_h) = |||u_h|||_\Omega^2.$$

This, together with weak convergence in V, completes the proof. □

3.2. First-order asymptotic expansion

Next, we seek the first-order asymptotic expansion of u_h^ϵ with respect to $\epsilon > 0$.

Remark 3 *Unfortunately, we may not expect convergence in the weak or strong topology of V. To see this, assume that there exists $0 \neq w \in V$ such that*

$$u_h^\epsilon = u_h + \theta(\epsilon) w + o(\theta(\epsilon)) \qquad \text{weakly in } V$$

for some smooth, strictly monotone function $\theta(\epsilon) : \mathbb{R}_0^+ \to \mathbb{R}_0^+$ with $\theta(0) = 0$. Since $V_h \subset V_h^\epsilon$ for all $\epsilon > 0$, we have, by Galerkin orthogonality,

$$a_\Omega(u_h^\epsilon - u_h, v_h) = 0 \qquad \forall\, v_h \in V_h$$

and therefore

$$a_\Omega\left(\frac{u_h^\epsilon - u_h}{\theta(\epsilon)}, v_h\right) = 0 \qquad \forall\, v_h \in V_h.$$

For $\epsilon \to 0$, we arrive at

$$a_\Omega(w, v_h) = 0 \qquad \forall\, v_h \in V_h. \tag{5}$$

Since, moreover, $(u_h^\epsilon - u_h)/\theta(\epsilon) \in V_h^\epsilon$, we have that $w \in V_h$ by Lemma 1 and hence we conclude that $w = 0$ is the unique solution of the homogeneous equation (5) in contradiction to the assumption. Let us emphasize that this observation holds true for any node insertion scenario, for which $V_h^\epsilon \subset V_h$ and the result of Lemma 1 can be proven. Apparently, this holds true for all cases a)–c) in Fig. 1.

Nevertheless, we have the following result:

Theorem 1 *Let u_h and u_h^ϵ be solutions of problems (P_h) and (P_h^ϵ), respectively. Then we have the following asymptotic expansion for $\epsilon \to 0$:*

$$u_h^\epsilon = u_h + \epsilon\,(y_h + y_s) + o(\epsilon) \qquad \begin{cases} \text{in } L^p(\Omega) \text{ for } 1 \leq p < \infty, \\ \text{in } H^1(\Omega \setminus \omega_E), \\ \text{weakly-}* \text{ in } BV(\Omega), \end{cases} \tag{6}$$

where

$$y_h \in V_h : \quad a_\Omega(y_h, v_h) = \sigma_{i_0,i_+} \langle z_{i_0,i_+}, v_h \rangle_V \quad \forall\, v_h \in V_h, \tag{7}$$

$$y_s = \sigma_{i_0,i_+}\, \varphi_{i_0} \chi_{\omega_E} \in BV(\Omega), \tag{8}$$

and

$$z_{i_0,i_+} = -\overline{a}_{\omega_E}(\,.\,, \varphi_{i_+}) - a_{\omega_E}(\,.\,, \varphi_{i_0}) \in V', \tag{9}$$

$$\sigma_{i_0,i_+} = \frac{(f, \varphi_{i_0})_{\omega_E} - \overline{a}_{\omega_E}(\varphi_{i_+}, u_h) - a_{\omega_E}(\varphi_{i_0}, u_h)}{\overline{a}_{\omega_E}(\varphi_{i_+}, \varphi_{i_+})} \in \mathbb{R}, \tag{10}$$

with $\overline{a}_{\omega_E}(u_h, v_h) := \displaystyle\int_\Omega \boldsymbol{K}_{i_0,i_+} \nabla u_h \cdot \nabla v_h \,\mathrm{d}x$ *and* $\boldsymbol{K}_{i_0,i_+}$ *defined in* (2).

Theorem 1 states that the first-order asymptotic expansion of u_h^ϵ is composed of a *singular* part $y_s \in BV(\Omega)$, arising from the degeneration of the basis function in the limit (1), and a *regular* part $y_h \in V_h$, which is given as a dual solution. However, since $y_h + y_s \notin V$, we may not dream of convergence in any topology of V, which has already been anticipated by Remark 3 above. Furthermore, it is also easy to see that the element-wise convergence to the discontinuous limit, e.g. in the broken space $H^1(\mathcal{T}_h) := \bigoplus_{T\in\mathcal{T}_h} H^1(T)$, can not hold.

Proof of Theorem 1. Due to the discrete nature of the problem, the proof boils down to the asymptotic analysis of the underlying finite-dimensional system: using the representations

$$u_h = \sum_{j=1}^N \mathrm{u}_j \varphi_j, \qquad u_h^\epsilon = \sum_{j=1}^N \mathrm{u}_j^\epsilon \varphi_j + \mathrm{u}_{i_\epsilon}^\epsilon \varphi_{i_\epsilon}^\epsilon,$$

we make the problem (P_h) equivalent to the N-dimensional linear system

$$\mathbf{A}\mathbf{u} = \mathbf{f}, \tag{11}$$

with the unknown coefficient vector $\mathbf{u} = [\mathrm{u}_j]_{j=1}^N$ and the usual stiffness matrix and right hand side

$$\mathbf{A} = [a_\Omega(\varphi_j, \varphi_i)]_{i,j=1}^N, \qquad \mathbf{f} = [(f, \varphi_i)_\Omega]_{i=1}^N.$$

Analogously, problem (P_h^ϵ) is equivalent to the $(N+1)$-dimensional linear system

$$\begin{bmatrix} \mathbf{A} & \mathbf{b}^\epsilon \\ \mathbf{b}^{\epsilon,\top} & \mathrm{c}^\epsilon \end{bmatrix} \begin{bmatrix} \mathbf{u}^\epsilon \\ \mathrm{u}_{i_\epsilon}^\epsilon \end{bmatrix} = \begin{bmatrix} \mathbf{f} \\ \mathrm{g}^\epsilon \end{bmatrix}, \tag{12}$$

where $\mathbf{A} \in \mathbb{R}^{N\times N}$ and $\mathbf{f} \in \mathbb{R}^N$ are defined above and

$$\mathbf{b}^\epsilon = [a_\Omega(\varphi_{i_\epsilon}^\epsilon, \varphi_i)]_{i=1}^N, \qquad \mathrm{c}^\epsilon = a_\Omega(\varphi_{i_\epsilon}^\epsilon, \varphi_{i_\epsilon}^\epsilon), \qquad \mathrm{g}^\epsilon = (f, \varphi_{i_\epsilon}^\epsilon)_\Omega.$$

Noting that $\mathrm{c}^\epsilon = \mathcal{O}(\frac{1}{\epsilon})$, we multiply the last line of (12) by $\epsilon > 0$ to obtain an equivalent system and abbreviate $\tilde{\mathrm{c}}^\epsilon := \epsilon\, \mathrm{c}^\epsilon$. We are now looking for the first-order asymptotic expansion

$$\begin{bmatrix} \mathbf{u}^\epsilon \\ \mathrm{u}^\epsilon_{i_\epsilon} \end{bmatrix} = \begin{bmatrix} \mathbf{u}^0 \\ \mathrm{u}^0_{i_\epsilon} \end{bmatrix} + \epsilon \begin{bmatrix} \mathbf{u}^1 \\ \mathrm{u}^1_{i_\epsilon} \end{bmatrix} + o(\epsilon).$$

As an immediate consequence of Lemma 2, together with the fact that $\varphi^\epsilon_{i_\epsilon} \to \varphi_{i_0} \chi_{\omega_E} \notin V_h$ by (1), we find that $\mathbf{u}^0 = \mathbf{u}$ and $u^0_{i_\epsilon} = 0$. Further, considering the Schur complement system of (12), multiplying by $\frac{1}{\epsilon}$ and inserting (11), we obtain

$$\begin{aligned} \frac{1}{\epsilon}\left(\mathbf{A}\mathbf{u}^\epsilon - \mathbf{A}\mathbf{u}\right) = \frac{1}{\epsilon}\left(\mathbf{A}\mathbf{u}^\epsilon - \mathbf{f}\right) &= -\frac{1}{\epsilon}\mathrm{u}^\epsilon_{i_\epsilon}\, \mathbf{b}^\epsilon \\ \frac{1}{\epsilon}\,\mathrm{u}^\epsilon_{i_\epsilon} &= \frac{1}{\tilde{\mathrm{c}}^\epsilon}\left(\mathrm{g}^\epsilon - \mathbf{b}^\epsilon \cdot \mathbf{u}^\epsilon\right) \end{aligned}$$

Thus, in the limit $\epsilon \to 0$ we arrive at

$$\mathbf{A}\mathbf{u}^1 = -\mathrm{u}^1_{i_\epsilon}\, \mathbf{b}^0, \tag{13}$$

$$\mathrm{u}^1_{i_\epsilon} = \frac{1}{\tilde{\mathrm{c}}^0}\left(\mathrm{g}^0 - \mathbf{b}^0 \cdot \mathbf{u}\right), \tag{14}$$

where the limits $\mathbf{b}^0 = \lim_{\epsilon\to 0} \mathbf{b}^\epsilon$, $\tilde{\mathrm{c}}^0 = \lim_{\epsilon\to 0} \tilde{\mathrm{c}}^\epsilon$, $\mathrm{g}^0 = \lim_{\epsilon\to 0} \mathrm{g}^\epsilon$ are to be determined in the following. To this end, we observe that

$$\varphi^\epsilon_{i_\epsilon} = \begin{cases} \frac{1}{\epsilon}\,\varphi_{i_+} & \text{on } \omega^\epsilon_E, \\ \frac{1}{1-\epsilon}\,\varphi_{i_0} & \text{on } \omega^{1-\epsilon}_E, \\ 0 & \text{else,} \end{cases}$$

and thus decompose

$$\begin{aligned} \mathrm{b}^\epsilon_i &= a_\Omega(\varphi_i, \varphi^\epsilon_{i_\epsilon}) = a_{\omega_E}(\varphi_i, \varphi^\epsilon_{i_\epsilon}) \\ &= \frac{1}{\epsilon}\, a_{\omega^\epsilon_E}(\varphi_i, \varphi_{i_+}) + \frac{1}{1-\epsilon}\, a_{\omega^{1-\epsilon}_E}(\varphi_i, \varphi_{i_0}) \end{aligned} \tag{15}$$

for $i = 1, \ldots, N$. For the first term, we consider transformation onto the reference elements as introduced above, see Fig. 4; using Fubini's theorem as well as Lebesgue's differentiation theorem and recalling the definition of $\boldsymbol{K}_{i_0,i_+}$ in (2), one finds for $j = 1, \ldots, M_E$ that

$$\begin{aligned} \frac{1}{\epsilon}\, a_{T^\epsilon_j}(\varphi_i, \varphi_{i_+}) &= \frac{1}{\epsilon} \int_{\hat{T}^\epsilon_j} \left(\hat{\boldsymbol{K}}(\hat{x})\, \nabla\hat{\varphi}_i \cdot \nabla\hat{\varphi}_{i_+} + \hat{c}(\hat{x})\, \hat{\varphi}_i\, \hat{\varphi}_{i_+}\right) |D\hat{\boldsymbol{F}}_j|\, \mathrm{d}\hat{x} \\ &\xrightarrow{\epsilon\to 0} \int_{\hat{T}_j} \hat{\boldsymbol{K}}(\hat{x})\, \nabla\hat{\varphi}_i \cdot \nabla\hat{\varphi}_{i_+} |D\hat{\boldsymbol{F}}_j|\, \mathrm{d}\hat{x} \\ &= \int_{T_j} \boldsymbol{K}_{i_0,i_+}(x)\, \nabla\varphi_i \cdot \nabla\varphi_{i_+}\, \mathrm{d}x = \overline{a}_{T_j}(\varphi_i, \varphi_{i_+}), \end{aligned}$$

where $\hat{(\,.\,)} = (\,.\,)\circ\hat{\boldsymbol{F}}$. Here, we made also use of the facts that $\hat{\varphi}_{i_+}(0,\hat{x}_2) = 0$ and that $\nabla\hat{\varphi}_i$ is element-wise constant. Employing Lebesgue's convergence theorem for the second term in (15), we end up with

$$\mathrm{b}_i^0 = \overline{a}_{\omega_E}(\varphi_i,\varphi_{i_+}) + a_{\omega_E}(\varphi_i,\varphi_{i_0})$$

for $i = 1,\dots,N$. Similarly, we have

$$\begin{aligned}\tilde{\mathrm{c}}^\epsilon &= \epsilon\, a_\Omega(\varphi_{i_\epsilon},\varphi_{i_\epsilon}) = \epsilon\, a_{\omega_E}(\varphi_{i_\epsilon},\varphi_{i_\epsilon})\\ &= \frac{1}{\epsilon}\, a_{\omega_E^\epsilon}(\varphi_{i_+},\varphi_{i_+}) + \frac{\epsilon}{(1-\epsilon)^2}\, a_{\omega_E^{1-\epsilon}}(\varphi_{i_0},\varphi_{i_0}),\end{aligned}$$

and deduce by the same arguments as above that

$$\tilde{\mathrm{c}}^0 = \overline{a}_{\omega_E}(\varphi_{i_+},\varphi_{i_+}).$$

Finally, since $\varphi_{i_\epsilon}^\epsilon \to \varphi_{i_0}\chi_{\omega_E}$ in $L^2(\Omega)$ as $\epsilon\to 0$, we get

$$\mathrm{g}^0 = (f,\varphi_{i_0})_{\omega_E}.$$

Now, we set $\sigma_{i_0,i_+} := \mathrm{u}_{i_\epsilon}^1$ and define $z_{i_0,i_+}\in V'$ such that $\langle z_{i_0,i_+},\varphi_i\rangle = -\mathrm{b}_i^0$, which yields (9)–(10). Furthermore, introducing

$$\begin{aligned}y_h &:= \sum_{j=1}^N \mathrm{u}_j^1\varphi_j \in V_h,\\ y_s &:= \mathrm{u}_{i_\epsilon}^1\,\varphi_{i_0}\chi_{\omega_E} \in BV(\Omega),\end{aligned}$$

we find, in particular, that (13)–(14) are equivalent to (7)–(8). Finally, we observe that

$$\frac{u_h^\epsilon - u_h}{\epsilon} = \sum_{j=1}^N \frac{\mathrm{u}_j^\epsilon - \mathrm{u}_j}{\epsilon}\varphi_j + \frac{\mathrm{u}_{i_\epsilon}^\epsilon}{\epsilon}\varphi_{i_\epsilon}^\epsilon,$$

and recall the convergence properties of $\varphi_{i_\epsilon}^\epsilon$ asserted in (1) to prove (6). □

3.3. Topological derivative of a functional

In view of the application we have in mind, the following result for differentiable $J: L^2(\Omega)\to\mathbb{R}$ will be sufficient. More general applications will be discussed in the subsequent remark.

THEOREM 2 *Let $J: L^2(\Omega)\to\mathbb{R}$ be Fréchet-differentiable in u_h with derivative $dJ(u_h)\in L^2(\Omega)'$. Then,*

$$D_{i_0,i_+}J(u_h) = \sigma_{i_0,i_+}\big(\langle z_{i_0,i_+},p_h\rangle_V + \langle dJ(u_h),\varphi_{i_0}\chi_{\omega_E}\rangle_{L^2(\Omega)}\big), \tag{16}$$

where $p_h\in V_h$ is given as the solution of the adjoint equation

$$a_\Omega(v_h,p_h) = \langle dJ(u_h),v_h\rangle_{L^2(\Omega)} \quad \forall\, v_h\in V_h \tag{17}$$

and $z_{i_0,i_+}\in V'$ and $\sigma_{i_0,i_+}\in\mathbb{R}$ are defined above in (9)–(10).

Proof Relying on Definition 1, the results from Theorem 1 and the definition of the adjoint solution $p_h \in V_h$ in (17), one obtains by the use of the chain rule and straightforward calculation

$$\begin{aligned} D_{i_0,i_+} J(u_h) &= \lim_{\epsilon \to 0} \frac{J(u_h^\epsilon) - J(u_h)}{\epsilon} \\ &= \langle dJ(u_h), y_h \rangle_{L^2(\Omega)} + \langle dJ(u_h), y_s \rangle_{L^2(\Omega)} \\ &= a_\Omega(y_h, p_h) + \langle dJ(u_h), y_s \rangle_{L^2(\Omega)} \\ &= \sigma_{i_0,i_+} \big(\langle z_{i_0,i_+}, p_h \rangle_V + \langle dJ(u_h), \varphi_{i_0} \chi_{\omega_E} \rangle_{L^2(\Omega)} \big). \end{aligned}$$

□

Remark 4 *In order to measure gradient and trace information in practical applications, the topological mesh derivative for general objective functions $J : V \to \mathbb{R}$ is, of course, desired. Unfortunately, in view of the insufficient convergence* (6) *due to the singular contribution $y_s \in BV(\Omega)$, a formula in the sense of Theorem 2 can not be deduced directly in general. Nevertheless, the derivation of $D_{i_0,i_+} J(u_h)$ for functionals involving gradients seems to be possible in many cases: for instance, this includes functionals of the form*

$$J(u) = \int_\Omega \boldsymbol{b}(x) \cdot \nabla u \, \mathrm{d}x$$

if $\boldsymbol{b}$ is continuous (or even piecewise continuous, using a more careful analysis based on the arguments above). Furthermore, if $J \in V'$ is of local character, such as evaluation of boundary values or integrals over small regions, $D_{i_0,i_+} J(u_h)$ can at least be easily obtained for all edges E outside those areas. For more demanding situations, additional analysis or a suitable approximation of J is needed.

Remark 5 *In comparison with goal-oriented refinement by the DWR-method (see Bangerth and Rannacher, 2003), note that the topological mesh derivative also depends on the solution $p_h \in V_h$ of an adjoint equation, which is independent of the chosen edge $E = (\boldsymbol{x}_{i_0}, \boldsymbol{x}_{i_+})$. In addition, it will be seen from the lines of the following section that the factors σ_{i_0,i_+} essentially provide information about the local residual. For further comments and perspectives in goal-oriented refinement see Section 6.*

4. Application to adaptive refinement

4.1. Minimization of the energy error

As a basic application of the concept of the topological mesh derivative, we consider the total potential energy

$$J_e(u) := \frac{1}{2} a_\Omega(u, u) - (f, u)_\Omega \tag{18}$$

corresponding to problem (P). As mentioned above, the total potential energy has been employed as a objective function for mesh optimization (r-adaptivity) by Delfour et al. (1985) and others, due to its direct relation to the energy error: in fact, relying on the symmetry of $a_\Omega(\,.\,,\,.\,)$ and Galerkin orthogonality, one easily derives

$$\begin{aligned}|||u_h^\epsilon - u|||_\Omega^2 &= a_\Omega(u_h^\epsilon - u, u_h^\epsilon - u)\\ &= a_\Omega(u_h^\epsilon, u_h^\epsilon) - 2a_\Omega(u, u_h^\epsilon) + a_\Omega(u,u)\\ &= a_\Omega(u_h^\epsilon, u_h^\epsilon) - 2(f, u_h^\epsilon)_\Omega - (a_\Omega(u,u) - 2(f,u)_\Omega)\\ &= 2(J_e(u_h^\epsilon) - J_e(u)),\end{aligned}$$

and analogously $|||u_h - u|||_\Omega^2 = 2(J_e(u_h) - J_e(u))$. By combining these equations, we obtain the crucial identity

$$|||u_h^\epsilon - u|||_\Omega^2 - |||u_h - u|||_\Omega^2 = 2\,(J_e(u_h^\epsilon) - J_e(u_h))\,. \tag{19}$$

Hence, $D_{i_0,i_+} J_e(u_h)$ can be regarded as a local sensitivity for minimizing the (quadratic) energy error by node insertion. Note, however, that identity (19) is limited to linear and symmetric elliptic equations. Using the results from the previous section, we immediately obtain the following formula:

COROLLARY 1 *For the total potential energy J_e defined in* (18) *we have*

$$D_{i_0,i_+} J_e(u_h) = -\frac{|(f,\varphi_{i_0})_{\omega_E} - \overline{a}_{\omega_E}(u_h,\varphi_{i_+}) - a_{\omega_E}(u_h,\varphi_{i_0})|^2}{2\,\overline{a}_{\omega_E}(\varphi_{i_+},\varphi_{i_+})}. \tag{20}$$

Proof Since $u_h \in V_h$ solves (P_h), we have

$$J_e(u_h) = \frac{1}{2}\,a_\Omega(u_h,u_h) - (f,u_h)_\Omega = -\frac{1}{2}\,(f,u_h)_\Omega$$

such that $\langle dJ_e(u_h), .\rangle_{L^2(\Omega)} = -\frac{1}{2}(f,\,.\,)_\Omega$, and, in particular, $p_h = -\frac{1}{2}\,u_h \in V_h$, as $a_\Omega(\,.\,,\,.\,)$ is symmetric and bilinear. Employing Theorem 2 and using once more the symmetry of $a_\Omega(\,.\,,\,.\,)$, we deduce

$$\begin{aligned}D_{i_0,i_+} J_e(u_h) &= -\frac{\sigma_{i_0,i_+}}{2}\big(\langle z_{i_0,i_+}, u_h\rangle_V + (f,\varphi_{i_0})_{\omega_E}\big)\\ &= -\frac{\sigma_{i_0,i_+}}{2}\big((f,\varphi_{i_0})_{\omega_E} - \overline{a}_{\omega_E}(\varphi_{i_+},u_h) - a_{\omega_E}(\varphi_{i_0},u_h)\big)\\ &= -\frac{|(f,\varphi_{i_0})_{\omega_E} - \overline{a}_{\omega_E}(u_h,\varphi_{i_+}) - a_{\omega_E}(u_h,\varphi_{i_0})|^2}{2\,\overline{a}_{\omega_E}(\varphi_{i_+},\varphi_{i_+})}.\end{aligned}$$

□

REMARK 6 *Note that in this case a computational evaluation of p_h is not required due to self-adjointness. Furthermore, we observe that $D_{i_0,i_+} J_e(u_h) \le 0$ for any edge $E = (\boldsymbol{x}_{i_0}, \boldsymbol{x}_{i_+})$. This observation confirms our expectation that insertion of nodes will decrease the error in the energy norm.*

4.2. Definition of a refinement indicator

In order to apply this result to adaptive refinement, let us define a local refinement indicator ι_E based on $D_{i_0,i_+}J_e(u_h)$. In view of (19), we would like to refine edges where $|D_{i_0,i_+}J_e(u_h)| = -D_{i_0,i_+}J_e(u_h)$ is large. Moreover, note that there are two distinct sensitivities per edge for the insertion of a node, namely $D_{i_0,i_+}J_e(u_h)$ and $D_{i_+,i_0}J_e(u_h)$. Hence, we define:

Definition 2 *For any interior edge $E = (\boldsymbol{x}_{i_0}, \boldsymbol{x}_{i_+}) \in \mathcal{E}_h^\Omega$, the refinement indicator based on the topological mesh derivative for the total potential energy is defined as*

$$\begin{aligned}\iota_E &:= \max\{|D_{i_0,i_+}J_e(u_h)|, |D_{i_+,i_0}J_e(u_h)|\} \\ &= \max_{\substack{j,k\in\{i_0,i_+\}\\ j\neq k}} \frac{|(f,\varphi_j)_{\omega_E} - \overline{a}_{\omega_E}(u_h,\varphi_k) - a_{\omega_E}(u_h,\varphi_j)|^2}{2\,\overline{a}_{\omega_E}(\varphi_k,\varphi_k)}.\end{aligned} \tag{21}$$

Remark 7 *As mentioned above, the resulting indicator is connected to the so-called correction indicators introduced by Zienkiewicz et al. (1983). Following the lines of the rigorous treatment of Aguilar and Goodman (2006), one finds the following representation for the error reduction for edge refinement with finite $0 < \epsilon < 1$:*

$$|||u_h - u|||_\Omega^2 - |||u_h^\epsilon - u|||_\Omega^2 = \frac{|(f,\varphi_{i_\epsilon}^\epsilon)_\Omega - a_\Omega(u_h,\varphi_{i_\epsilon}^\epsilon)|^2}{\inf_{v_h\in V_h} |||v_h - \varphi_{i_\epsilon}^\epsilon|||_\Omega^2} \tag{22}$$

The correction indicators are then constructed by replacing V_h by $W_0 := \{0\}$ as in Zienkiewicz et al. (1983) or by $W_4 := \mathrm{lin}\{\varphi_j \in V_h : \boldsymbol{x}_j \in \partial\omega_E\}$ as proposed by Aguilar and Goodman (2006) in two space dimensions. Considering Poisson's equation as a model problem, Aguilar and Goodman (2006) prove that both versions are effective in the sense that the true error reduction (22) *can be bounded from above and below in terms of the indicators, where the constants depend on the shape of the neighboring elements $T \in \omega_E$. Note that the latter version involves the solution of a small subproblem, but appears to be much more reliable in case of ill-shaped neighboring elements occurring in applications to anisotropic refinement, see Aguilar and Goodman (2006) for details.*

In fact, it is easy to see that $D_{i_0,i_+}J_e(u_h)$ and hence ι_E could also be obtained from the identity (22)*, using the arguments from the proof of Theorem 1.*

4.3. Relationship to residual-based error estimator

For the discussion in the remainder of this section, we confine ourselves to $d = 2$ and require that the coefficient function $\boldsymbol{K} \equiv \overline{\boldsymbol{K}}$ be element-wise constant. In order to examine the quality of the refinement indicator ι_E, we consider the classical residual-based error estimator η_E which reads in this case as (see Verfürth, 1996; Ainsworth and Oden, 2000, and, in particular, Brenner and

Scott, 2002; Morin et al., 2000, for the edge-wise representation)

$$\eta_E^2 := \sum_{T \subset \omega_E} h_T^2 \|r\|_T^2 + h_E \|j_E\|_E^2, \tag{23}$$

where the jump and element residuals are given by

$$j_E := [\![\overline{\boldsymbol{K}} \nabla u_h \cdot \boldsymbol{n}_E]\!]_E, \qquad r := f - cu_h,$$

independently of the direction of the normal $\boldsymbol{n}_E$ on edge E, and we may take

$$h_T = |T|^{1/2}, \qquad h_E = |E|$$

for shape regular triangulations $\mathcal{T}_h$. Furthermore, we recall the well-known global upper and local lower bound of the energy error in terms of the estimators η_E (see Verfürth, 1996; Ainsworth and Oden, 2000),

$$|||u - u_h|||_\Omega^2 \le C \sum_{E \in \mathcal{E}_h^\Omega} \eta_E^2, \tag{24}$$

$$\eta_E^2 \le C_1 |||u - u_h|||_{\omega_E}^2 + C_2 \sum_{T \subset \omega_E} h_T^2 \|r - \overline{r}_T\|_T^2, \tag{25}$$

where $\overline{r}_T$ is the mean value of r on T, and the constants are only depending on the smallest angle in the triangulation and the eigenvalues of $\overline{\boldsymbol{K}}$. We are now in the position to state the following important result on the relation between ι_E and the classical residual-based error indicator:

THEOREM 3 *Let $d = 2$ and assume that the coefficient function $\boldsymbol{K} \equiv \overline{\boldsymbol{K}}$ is element-wise constant.*

a) For any interior edge $E \in \mathcal{E}_h^\Omega$, we have

$$\iota_E \le C\, \eta_E^2. \tag{26}$$

b) For any interior node $\boldsymbol{x}_{i_0} \in \mathcal{N}_h^\Omega$, $1 \le i_0 \le N$, define the patch

$$\tilde{\omega}_0 := \bigcup_{\substack{\boldsymbol{x}_{i_0} \in \partial T \\ T \in \mathcal{T}_h}} T \tag{27}$$

and the star-graph $\tilde{\gamma}_0 := \{E \in \mathcal{E}_h^\Omega : \boldsymbol{x}_{i_0} \in \partial E\}$ of edges in $\tilde{\omega}_0$ sharing node $\boldsymbol{x}_{i_0}$. Then,

$$\sum_{E \subset \tilde{\gamma}_0} \eta_E^2 \le C_1 \sum_{E \subset \tilde{\gamma}_0} \iota_E + C_2\, h_{\tilde{\omega}_0}^2 \|r - \overline{r}_{\tilde{\omega}_0}\|_{\tilde{\omega}_0}^2, \tag{28}$$

where $h_{\tilde{\omega}_0} = |\tilde{\omega}_0|^{1/2}$ and $\overline{r}_{\tilde{\omega}_0}$ is the mean value of r on $\tilde{\omega}_0$.

Here, the constants $C, C_1, C_2 > 0$ only depend on the smallest angle in the triangulation $\mathcal{T}_h$ and the minimal and maximal eigenvalues of $\overline{\boldsymbol{K}}$.

We postpone the proof of Theorem 3 to the end of this section. The following result is an immediate consequence of Theorem 3 and the lower and upper bounds (24), (25):

Corollary 2 *Under the assumptions of Theorem 3, the following estimates are true:*

a)

$$\iota_E \leq C_1 |||u - u_h|||^2_{\omega_E} + C_2 \sum_{T \subset \omega_E} h_T^2 \|r - \overline{r}_T\|_T^2 \qquad \forall E \in \mathcal{E}_h^\Omega \tag{29}$$

b)

$$|||u - u_h|||^2_\Omega \leq C_3 \sum_{E \in \mathcal{E}_h^\Omega} \iota_E + C_4 \sum_{1 \leq i \leq N} h^2_{\tilde{\omega}_i} \|r - \overline{r}_{\tilde{\omega}_i}\|^2_{\tilde{\omega}_i}. \tag{30}$$

Here, the constants $C_1, C_2, C_3, C_4 > 0$ only depend on the smallest angle in the triangulation $\mathcal{T}_h$ and the minimal and maximal eigenvalues of $\overline{\boldsymbol{K}}$, and $\tilde{\omega}_i$ are the patches associated with the interior nodes $\boldsymbol{x}_i \in \mathcal{N}_h^\Omega$ as defined in (27).

Remark 8 *Several remarks on Theorem 3 and Corollary 2 are in order:*

- *We may conclude from Theorem 3, that the sensitivity-based refinement indicator ι_E is patch-wise equivalent to the classical residual-based error estimator η_E^2 up to oscillations $h^2_{\tilde{\omega}_0} \|r - \overline{r}_{\tilde{\omega}_0}\|^2_{\tilde{\omega}_0}$, which are expected to be of higher order (see Morin et al., 2000). In particular, ι_E depends on the same residual contributions with the same asymptotically accurate weights in terms of edge and element sizes. Hence, we may presume that the proposed indicator might perform similarly in an adaptive algorithm. Recall, however, that the derivations of these indicators are based on completely different motivations: in view of* (19)*, the indicator ι_E is constructed to be a local sensitivity for minimization of the (quadratic) error rather than an estimator for the actual local error itself. On the other hand, this result confirms that the explicit residual-based (and any equivalent) error estimator leads to efficient adaptive refinement in the sense that it is locally equivalent to sensitivities for error reduction.*
- *As a consequence of Theorem 3, the indicator ι_E is equivalent to the error in the sense of Corollary 2. Hence, we conclude from* (29) *that if ι_E is large, the local error on ω_E is also large. On the other hand,* (30) *asserts that $\sum_{E \in \mathcal{E}_h} \iota_E$ does not vanish unless $u = u_h$, at least in the case of sufficiently nice data. However, aside from this observation, the result of Corollary 2 does not imply a reliable quantitative relation in the sense of error estimation. Since ι_E is based on edge-wise sensitivities rather than estimates on the local error itself, the value $\sum_{E \in \mathcal{E}_h} \iota_E$ does not allow for any meaningful interpretation with regard to the global energy error $|||u - u_h|||_\Omega$. In fact, as can be seen from the numerical examples below, the values of ι_E are indeed on a smaller scale than the local errors. With*

this in mind, we emphasize once more that the derived indicator is not appropriate for error evaluation and error control. Accordingly, a precise estimation of the error in terms of ι_E, including a more careful analysis for the constants appearing in Corollary 2, is not our primary attempt.

- *Note that the indicator ι_E does not capture the fine data variations within elements. In particular, additional error contributions, corresponding to data oscillations, appear in both bounds* (29) *and* (30)*. Anyway, it is well-known that data oscillations play a crucial role in adaptivity in general, as they have to be considered in addition, in order to ensure convergence of the adaptive algorithm even for typical error estimators (Morin et al., 2000, 2008). Therefore, one should, for instance, include oscillation indicators in the marking strategy.*
- *Our proof utilizes the restriction to element-wise constant $\boldsymbol{K}$ as well as the linearity of shape functions $\{\varphi_j\}_{j=1}^N$ on several occasions, e.g. for the derivation of the crucial identity* (31)*. In fact, the generalization of the results of Theorem 3 in the case of non-constant $\boldsymbol{K}$ seems to be elaborate, even if oscillations for the jump residuals are taken into account. Regarding higher-order elements, note that the details of the refinement procedure will differ and the asymptotic analysis will lead to a different formula for ι_E in the first place.*

Proof of Theorem 3 Due to the assumption that $\boldsymbol{K} \equiv \overline{\boldsymbol{K}}$ is element-wise constant, we may rewrite

$$(f, \varphi_{i_0})_{\omega_E} - \overline{a}_{\omega_E}(u_h, \varphi_{i_+}) - a_{\omega_E}(u_h, \varphi_{i_0}) = (r, \varphi_{i_0})_{\omega_E} - \overline{a}_{\omega_E}(u_h, \varphi_{i_0} + \varphi_{i_+}).$$

For the first term on the right hand side, we observe that

$$\nabla(\varphi_{i_0} + \varphi_{i_+})|_T = \frac{|E|}{2\,|T|}\boldsymbol{n}_{E,T},$$

where $\boldsymbol{n}_{E,T}$ is the normal on E pointing outward from T. Hence, by exploiting the fact that $\overline{\boldsymbol{K}}\,\nabla u_h$ is constant on $T \subset \omega_E$, we obtain the crucial ingredient

$$\begin{aligned} \overline{a}_{\omega_E}(u_h, \varphi_{i_0} + \varphi_{i_+}) &= \sum_{T \subset \omega_E} \int_T \overline{\boldsymbol{K}}\,\nabla u_h \cdot \nabla(\varphi_{i_+} + \varphi_{i_0})\,\mathrm{d}x \\ &= \frac{1}{2}\int_E [\![\overline{\boldsymbol{K}}\,\nabla u_h \cdot \boldsymbol{n}_E]\!]_E\,\mathrm{d}x = \frac{1}{2}\int_E j_E\,\mathrm{d}x. \end{aligned} \tag{31}$$

Furthermore, observe that

$$\overline{c}_a \le \frac{1}{\overline{a}_{\omega_E}(\varphi_j, \varphi_j)} \le \overline{C}_a, \qquad j = i_0, i_+,$$

uniformly for all edges $E \in \mathcal{E}_h^\Omega$, where the constants $\overline{c}_a, \overline{C}_a > 0$ only depend on the smallest angle in the triangulation $\mathcal{T}_h$ and the minimal and maximal

eigenvalues of $\overline{\boldsymbol{K}}$. In the following, the constants $C, C_1, C_2, \ldots$ may depend on these bounds and may – as usual – change their values on different occurrences within one estimate.

To prove the first result, (26), we may simply employ Young's and Cauchy-Schwarz inequalities to estimate

$$\begin{aligned}
\iota_E &= \max\{|D_{i_0,i_+} J_e(u_h)|, |D_{i_+,i_0} J_e(u_h)|\} \\
&\leq \overline{C}_a \max_{j\in\{i_0,i_+\}} |(r,\varphi_j)_{\omega_E} - \overline{a}_{\omega_E}(u_h, \varphi_{i_0} + \varphi_{i_+})|^2 \\
&\leq C_1 \max_{j\in\{i_0,i_+\}} \sum_{T\subset\omega_E} \|r\|_T^2 \|\varphi_j\|_{\omega_E}^2 + C_2 |\overline{a}_{\omega_E}(u_h, \varphi_{i_0} + \varphi_{i_+})|^2 \\
&\leq C_1 \sum_{T\subset\omega_E} h_T^2 \|r\|_T^2 + C_2 h_E \|j_E\|_E^2 \\
&\leq C\, \eta_E^2.
\end{aligned}$$

For the proof of the second statement, (28), let us fix an arbitrary $\boldsymbol{x}_{i_0} \in \mathcal{N}_h^\Omega$, $1 \leq i_0 \leq N$, and enumerate the nodes $\{\boldsymbol{x}_{i_k}\}_{i_k=1}^{M_0} \subset \partial\tilde{\omega}_0$ for some $M_0 \in \mathbb{N}$, and consider the corresponding edges $E_k = (\boldsymbol{x}_{i_0}, \boldsymbol{x}_{i_k}) \in \tilde{\gamma}_0$ together with their neighborhoods $\omega_k = \omega_{E_k}$. For the second result to hold, an additional ingredient is needed in order to ensure that the two terms within the absolute value do not cancel. This is achieved by the following estimate:

$$\begin{aligned}
\sum_{E\in\tilde{\gamma}_0} \iota_E &= \sum_{k=1}^{M_0} \max\{|D_{i_0,i_k} J_e(u_h)|, |D_{i_k,i_0} J_e(u_h)|\} \\
&\geq \frac{\overline{c}_a}{2} \sum_{k=1}^{M_0} \sum_{l=i_0,i_k} |(r,\varphi_l)_{\omega_k} - \overline{a}_{\omega_k}(u_h, \varphi_{i_0} + \varphi_{i_k})|^2 \qquad (32) \\
&\geq \frac{\overline{c}_a}{4M_0} |\sum_{k=1}^{M_0} (r, \varphi_{i_0} + \varphi_{i_k})_{\omega_k} - 2\,\overline{a}_{\omega_k}(u_h, \varphi_{i_0} + \varphi_{i_k})|^2.
\end{aligned}$$

For convenience, we introduce $\psi_{i_0} = \chi_{\tilde{\omega}_0} \sum_{k=1}^{M_0} \varphi_{i_k} = \chi_{\tilde{\omega}_0} - \varphi_{i_0}$ and observe that

$$\begin{aligned}
\sum_{k=1}^{M_0} \overline{a}_{\omega_k}(u_h, \varphi_{i_0}) &= \sum_{k=1}^{M_0} \sum_{T\in\omega_k} \overline{a}_T(u_h, \varphi_{i_0}) = 2\,\overline{a}_{\tilde{\omega}_0}(u_h, \varphi_{i_0}), \\
\sum_{k=1}^{M_0} \overline{a}_{\omega_k}(u_h, \varphi_{i_k}) &= \overline{a}_{\tilde{\omega}_0}(u_h, \psi_{i_0}) = -\overline{a}_{\tilde{\omega}_0}(u_h, \varphi_{i_0}),
\end{aligned}$$

and furthermore

$$\sum_{k=1}^{M_0} \big(\overline{a}_{\omega_k}(u_h, \varphi_{i_0}) - (r, \varphi_{i_0})_{\omega_k}\big) = 2\big(a_\Omega(u_h, \varphi_{i_0}) - (f, \varphi_{i_0})_\Omega\big) = 0.$$

Thus, (32) results in

$$|(r,\psi_{i_0})_{\tilde\omega_0}|^2 \le CM_0 \sum_{E\in\tilde\gamma_0} \iota_E, \tag{33}$$

and it remains to bound η_E^2 in terms of the left hand side of (33). Computing

$$\int_{\tilde\omega_0} \psi_{i_0}\,\mathrm{d}x = \tfrac{2}{3}|\tilde\omega_0|, \qquad \|\psi_{i_0}\|^2_{\tilde\omega_0} = \tfrac{1}{2}|\tilde\omega_0|,$$

we proceed by estimating

$$\begin{aligned}
\sum_{E\in\tilde\gamma_0}\sum_{T\subset\omega_E} h_T^2\|r\|_T^2 = 2\sum_{T\in\tilde\omega_0} h_T^2\|r\|_T^2 &\le 2\max_{T\subset\tilde\omega_0} h_T^2\|r\|^2_{\tilde\omega_0}\\
&\le C_1 \max_{T\subset\tilde\omega_0} h_T^2\|\overline{r}_{\tilde\omega_0}\|^2_{\tilde\omega_0} + C_2 h^2_{\tilde\omega_0}\|r-\overline{r}_{\tilde\omega_0}\|^2_{\tilde\omega_0}\\
&\le C_1 \max_{T\subset\tilde\omega_0} \frac{h_T^2}{h^2_{\tilde\omega_0}}|(\overline{r}_{\tilde\omega_0},\psi_{i_0})_{\tilde\omega_0}|^2 + C_2 h^2_{\tilde\omega_0}\|r-\overline{r}_{\tilde\omega_0}\|^2_{\tilde\omega_0}\\
&\le C_1 \max_{T\subset\tilde\omega_0} \frac{h_T^2}{h^2_{\tilde\omega_0}}|(r,\psi_{i_0})_{\tilde\omega_0}|^2 + C_2 h^2_{\tilde\omega_0}\|r-\overline{r}_{\tilde\omega_0}\|^2_{\tilde\omega_0}.
\end{aligned} \tag{34}$$

On the other hand, recalling (31) and repeating the preceding arguments,

$$\begin{aligned}
\sum_{E\in\tilde\gamma_0} h_E\|j_E\|_E^2 &= 4\sum_{k=1}^{M}|\overline{a}_{\omega_k}(u_h,\varphi_{i_0}+\varphi_{i_k})|^2\\
&\le C_1\sum_{E\in\tilde\gamma_0}|D_{i_0,i_k}J_e(u_h)| + C_2\sum_{E\in\tilde\gamma_0}|(r,\varphi_{i_0})_{\omega_E}|^2\\
&\le C_1\sum_{E\in\tilde\gamma_0}\iota_E + C_2\max_{T\subset\tilde\omega_0} h_T^2\|r\|^2_{\tilde\omega_0}\\
&\le C_1\sum_{E\in\tilde\gamma_0}\iota_E + C_2\max_{T\subset\tilde\omega_0}\frac{h_T^2}{h^2_{\tilde\omega_0}}|(r,\psi_{i_0})_{\omega_E}|^2 + C_3 h^2_{\tilde\omega_0}\|r-\overline{r}_{\tilde\omega_0}\|^2_{\tilde\omega_0}.
\end{aligned} \tag{35}$$

Finally, we combine the previous estimates (33), (34) and (35) and observe that

$$M_0\max_{T\in\tilde\omega_0}\frac{h_T^2}{h^2_{\tilde\omega_0}} \le \frac{\max_{T\in\tilde\omega_0} h_T^2}{\min_{T\in\tilde\omega_0} h_T^2} \le C,$$

where the constant only depends on the shape regularity of $\mathcal{T}_h$. This completes the proof. □

5. Numerical experiments

Let us examine the quality of ι_E in two numerical experiments in $d = 2$.

5.1. Adaptive algorithm

In the first test, we investigate the numerical performance of our concept of sensitivity-based mesh refinement in comparison to the classical approach of error-controlled adaptivity. To this end, we compare ι_E to the standard explicit residual-based error estimator η_E (23) as refinement indicators in an adaptive algorithm.[1]

The procedure is as follows: For η_E and ι_E, we consider two independent, initially equal meshes. First, the indicators η_E and ι_E are evaluated for all interior edges of their corresponding triangulations. We then mark edges for refinement by the maximum strategy (Babuška and Rheinboldt, 1978): for given $0 < \Theta \leq 1$, we determine the subsets of edges

$$\mathcal{M}_\eta = \{E : \eta_E^2 \geq \Theta \max_{E'} \eta_{E'}^2\}, \qquad \mathcal{M}_\iota = \{E : \iota_E \geq \Theta \max_{E'} \iota_{E'}\}.$$

In the examples below we choose $\Theta = 0.1$. Edges $E \in \mathcal{M}_\eta, \mathcal{M}_\iota$, respectively, are then marked for refinement on the corresponding meshes. The refinement is carried out by newest vertex bisection (NVB) (Mitchell, 1989) and we proceed with the next iteration on both refined meshes.

The experiments have been implemented and performed in MATLAB. For NVB-refinement, our implementation is based on some modules from Funken et al. (2011); the routines have been slightly modified in order to account for the edge-based rather than the element-based marking and refinement. By use of NVB-refinement, shape regularity of the families of refined triangulations is preserved throughout the algorithm.

REMARK 9 *Since ι_E is by construction an edge-based indicator, it seems to perform better if single edges are marked instead of all edges of adjacent elements. In this context, note that for elements with more than one marked edge refinement according to the derivation of ι_E, that is, by the process described in section 2.2, is neither possible nor wanted.*

REMARK 10 *The computation of ι_E only requires evaluations of given data and basis functions. Therefore, the computational costs for the evaluation of ι_E are comparable to those of η_E.*

5.2. Accuracy test

In the second experiment, we try to assess the reliability of ι_E as a local indicator for error reduction. Typically, the quality of a refinement indicator in a posteriori error estimation is addressed to by its *effectivity index*, which is measured as the ratio of estimator value to the true error (see Verfürth, 1996; Ainsworth and Oden, 2000). However, as discussed in Remark 8, we do not

[1] In this context, we refer to the studies and conclusions of Carstensen and Merdon (2010) on several a posteriori error estimators with regard to their similar performance as mesh refinement indicators.

expect an accurate relation between $\sum_{E\in\mathcal{E}_h^\Omega}\iota_E$ and $|||u-u_h|||_\Omega^2$. Rather, we shall examine the reliability of ι_E as a sensitivity by the ratio of the local indicator value (prediction) to the actual local error reduction. In particular, since the derivation of the sensitivities is based on infinitesimal small $\epsilon\to 0$, we are interested in the accuracy for practical refinement with finite $\epsilon=\frac{1}{2}$.

To this end, we evaluate ι_E for all interior edges on a uniformly refined mesh. Then, every edge is refined by bisection as in Fig. 2 with $\epsilon=\frac{1}{2}$. The reduction of the quadratic error

$$\Delta_E := |||u_h-u|||_\Omega^2 - |||u_h^{1/2}-u|||_\Omega^2 = 2\left(J_e(u_h)-J_e(u_h^{1/2})\right) \tag{36}$$

is evaluated and compared to the prediction ι_E. For the evaluation (36), we use the right hand side of (19), as it only depends on the discrete solutions. To avoid perturbations of the ratios by quantities close to zero, we exclude those samples from the results, for which both $\Delta_E<10^{-12}$ and $\iota_E<10^{-12}$ are true.

For comparison, we will also show the correlation between η_E^2 and Δ_E in order to explain a possibly superior adaptive performance of ι_E from this point of view. However, we emphasize that we do not expect any reliable connection between η_E^2 and Δ_E by construction. Vice versa, the quality of ι_E as an error estimator would of course be inferior to η_E.

5.3. Example 1: the crack problem

We consider Poisson's equation ($\boldsymbol{K}\equiv\boldsymbol{I}$, $c\equiv 0$) on the slit domain $\Omega=\{(x,y)\in\mathbb{R}^2:|x|+|y|<1\}\setminus([0,1]\times\{0\})$ with the constant right hand side $f\equiv 1$; the non-homogeneous Dirichlet boundary data are determined from the exact solution which is given in polar coordinates by

$$u(r,\theta)=r^{1/2}\sin(\theta/2)-\tfrac{1}{2}r^2\sin^2(\theta)$$

(see Morin et al., 2003; Carstensen and Merdon, 2010). The extension of our results to problems with non-homogeneous Dirichlet data is straightforward and one obtains the indicator ι_E literally as defined in Definition 2.

The adaptive algorithm creates a mesh with a fine resolution around the singularity of type $r^{1/2}$ at the origin, see Fig. 5 b). The performance of ι_E in adaptive refinement is apparently competitive in comparison to η_E as illustrated in Fig. 6. In the second test, we find that the prediction ι_E and the actual error decrease Δ_E are well correlated as demonstrated in Fig. 7 a). The relation between indicator value and actual error reduction for the residual-based estimator is depicted in Fig. 7 b) for comparison. We suppose that the slightly superior performance of our indicator in the adaptive algorithm can be explained by its better correlation to the error reduction. However, we stress that both indicators seem to be equally reliable for large local errors, whereas accuracy at small scales is rather irrelevant from the practical point of view.

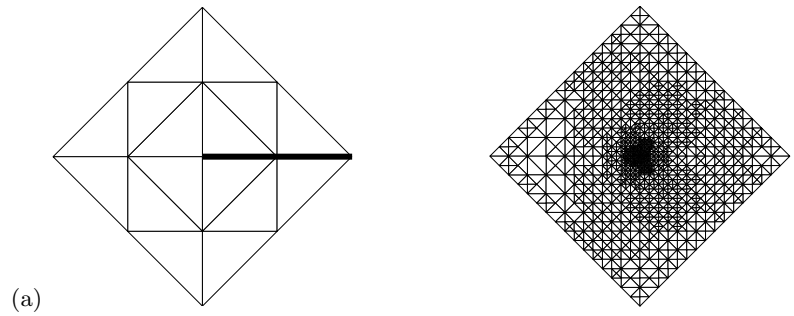

(a)

Figure 5. (a) Initial mesh ($N = 3$) for Example 1. The crack $[0, 1] \times \{0\}$ from the center to the right-hand corner is indicated by the bold line. (b) Locally refined mesh ($N = 1144$) generated by the adaptive algorithm based on ι_E

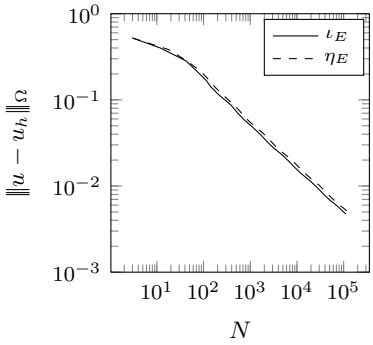

Figure 6. Adaptive algorithm for Example 1. Energy error $|||u - u_h|||_\Omega$ vs. number of degrees of freedom N on adaptively refinement meshes generated by ι_E (solid line) and η_E (dashed line)

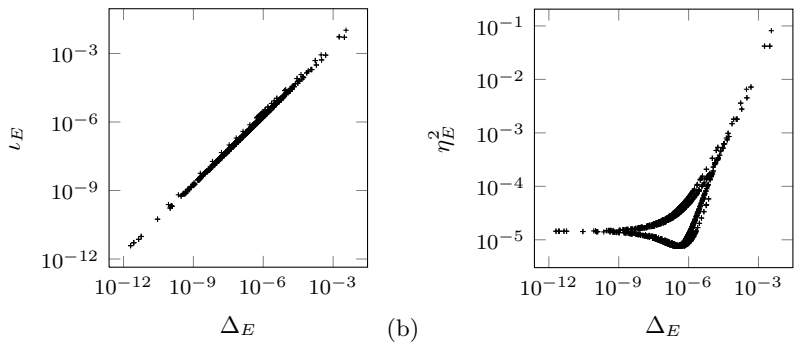

(a) (b)

Figure 7. Accuracy test for Example 1 on a uniform mesh ($N = 465$). Every mark corresponds to bisection of an edge $E \in \mathcal{E}_h^\Omega$. (a) Refinement indicator ι_E vs. reduction of the quadratic error Δ_E. (b) Residual-based error estimator η_E^2 vs. reduction of the quadratic error Δ_E for comparison

5.4. Example 2: the varying right hand side

In this example, let the exact solution to Poisson's problem ($\boldsymbol{K} \equiv \boldsymbol{I}$, $c \equiv 0$) on $\Omega = (0,1)^2$ with homogeneous Dirichlet data be given by

$$u(x,y) = x(x-1)\, y(y-1)\, \exp(-100\,(x-\tfrac{1}{2})^2 - 100\,(y-\tfrac{117}{1000})^2),$$

where the right hand side f is determined accordingly (see Luce and Wohlmuth, 2004; Carstensen and Merdon, 2010).

We confirm that our indicator is competitive in view of the results for the adaptive algorithm depicted in Fig. 9. Again, we suppose that the slightly better performance of our indicator is due to the fact that the correlation of error reduction and indicator value is better than for the residual-based error estimator, see Fig. 10. In comparison to the previous example, the ratios Δ_E/ι_E are perturbed by some outliers due to large oscillations on the rather coarse uniform mesh.

6. Conclusion and outlook

From the results above we may conclude that the sensitivity-based indicator ι_E appears to be competitive in adaptive refinement for minimization of the energy error. Consequently, in view of Theorem 2 and its generalizations in the sense of Remark 4, the concept of the topological mesh derivative seems to be suited for goal-oriented refinement. Note, however, that a relation between the topological mesh derivative and the error in terms of the discrete and unknown solutions – as given by (19) in the special case of the total potential energy – is in general not available.

Therefore, one may only calculate sensitivities for the evolution of the quantity $J(u_h)$ instead of the error $|J(u_h)-J(u)|$ that shall be minimized. Since $J(u)$ is mesh-independent, one might consider $|D_{i_0,i_+}J(u_h)|$ as an (unsigned) sensitivity for the error. Hence, in the absence of additional arguments or futher knowledge on J, one has to rely on the *assumption* that refinement will in fact decrease the error $|J(u_h)-J(u)|$. These issues will be addressed in a forthcoming publication.

Acknowledgments

The authors gratefully acknowledge the funding of the German Research Council (DFG), which, within the framework of its "Excellence Initiative" supports the Cluster of Excellence "Engineering of Advanced Materials" (www.eam.uni-erlangen.de) at the University of Erlangen-Nuremberg.

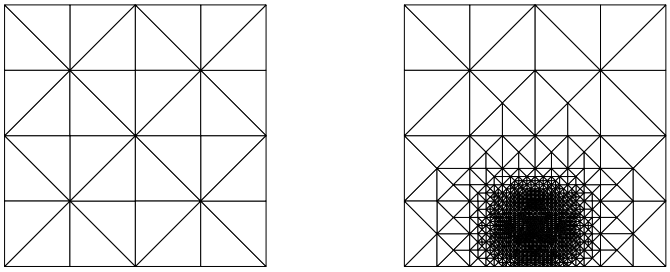

Figure 8. (a) Initial mesh ($N = 9$) for Example 2. (b) Locally refined mesh ($N = 1263$) generated by the adaptive algorithm based on ι_E

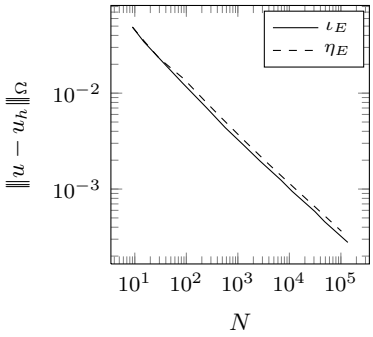

Figure 9. Adaptive algorithm for Example 2. Energy error $|||u - u_h|||_\Omega$ vs. number of degrees of freedom N on adaptively refinement meshes generated by ι_E (solid line) and η_E (dashed line).

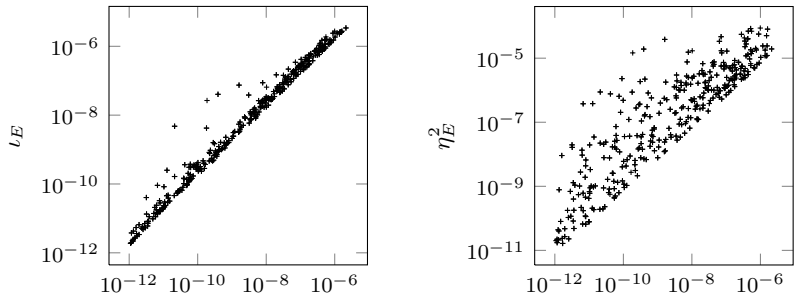

(a) (b)

Figure 10. Accuracy test for Example 2 on a uniform mesh ($N = 961$). Every mark corresponds to bisection of an edge $E \in \mathcal{E}_h^\Omega$. (a) Refinement indicator ι_E vs. reduction of the quadratic error Δ_E. (b) Residual-based error estimator η_E^2 vs. reduction of the quadratic error Δ_E for comparison

References

Aguilar, J. C. and Goodman, J. B. (2006) Anisotropic mesh refinement for finite element methods based on error reduction. *Journal of Computational and Applied Mathematics*, **193**(2), 497–515.

Ainsworth, M. and Oden, J. T. (2000) *A Posteriori Error Estimation in Finite Element Analysis*. Wiley, New York.

Alt, H. W. (2002) *Lineare Funktionalanalysis*. Springer, Berlin, 4th edition.

Ambrosio, L., Fusco, N., and Pallara, D. (2000) *Functions of Bounded Variation and Free Discontinuity Problems*. Oxford University Press, New York.

Babuška, I. and Aziz, A. K. (1976) On the angle condition in the finite element method. *SIAM Journal on Numerical Analysis*, **13**(2), 214–226.

Babuška, I. and Rheinboldt, W. C. (1978) Error estimates for adaptive finite element computations. *SIAM Journal on Numerical Analysis*, **15**(4), 736–754.

Bangerth, W. and Rannacher, R. (2003) *Adaptive Finite Element Methods for Differential Equations*. Birkhäuser, Basel.

Bank, R. E. (1996) Hierarchical bases and the finite element method. *Acta Numerica*, **5**, 1–45.

Bank, R. E. and Smith, R. K. (1993) A posteriori error estimates based on hierarchical bases. *SIAM Journal on Numerical Analysis*, **30**(4), 921–935.

Brenner, S. C. and Scott, L. R. (2002) *The Mathematical Theory of Finite Element Methods*. Springer, New York, 2nd edition.

Carstensen, C. and Merdon, C. (2010) Estimator competition for poisson problems. *Journal of Computational Mathematics*, **28**(3), 309–330.

Ciarlet, P. G. (2002) *The Finite Element Method for Elliptic Problems*. SIAM, Philadelphia, 2nd edition.

Delfour, M. C., Payre, G., and Zolésio, J.-P. (1985) An optimal triangulation for second-order elliptic problems. *Computer Methods in Applied Mechanics and Engineering*, **50**(3), 231–261.

Deuflhard, P., Leinen, P., and Yserentant, H. (1989) Concepts of an adaptive hierarchical finite element code. *IMPACT of Computing in Science and Engineering*, **1**(1), 3–35.

Friederich, J., Leugering, G., and Steinmann, P. (2012) Adaptive refinement based on asymptotic expansions of finite element solutions for node insertion in 1d. *GAMM-Mitteilungen*, **35**(2), 175–190.

Funken, S. A., Praetorius, D., and Wissgott, P. (2011) Efficient implementation of adaptive p1-fem in matlab. *Computational Methods in Applied Mathematics*, **11**(4), 460–490.

Krysl, P., Grinspun, E., and Schröder, P. (2003) Natural hierarchical refinement for finite element methods. *International Journal for Numerical Methods in Engineering*, **56**(8), 1109–1124.

Leugering, G. and Sokolowski, J. (2008) Topological sensitivity analysis for elliptic problems on graphs. *Control and Cybernetics*, **37**(4), 971–997.

Leugering, G. and Sokolowski, J. (2011) Topological derivatives for networks of elastic strings. *Zeitschrift für Angewandte Mathematik und Mechanik*, **91**(12), 926–943.

Luce, R. and Wohlmuth, B. (2004) A local a posteriori error estimator based on equilibrated fluxes. *SIAM Journal on Numerical Analysis*, **42**(4), 1394–1414.

Mitchell, W. F. (1989) A comparison of adaptive refinement techniques for elliptic problems. *ACM Transactions on Mathematical Software*, **15**(4), 210–227.

Morin, P., Nochetto, R. H., and Siebert, K. G. (2000) Data oscillation and convergence of adaptive fem. *SIAM Journal on Numerical Analysis*, **38**(2), 466–488.

Morin, P., Nochetto, R. H., and Siebert, K. G. (2003) Local problems on stars: a posteriori error estimators, convergence, and performance. *Mathematics of Computation*, **72**(243), 1067–1097.

Morin, P., Siebert, K. G., and Veeser, A. (2008) A basic convergence result for conforming adaptive finite elements. *Mathematical Methods in the Applied Sciences*, **18**(5), 707–737.

Novotny, A. A., Feijóo, R. A., Taroco, E., and Padra, C. (2003) Topological sensitivity analysis. *Computer Methods in Applied Mechanics and Engineering*, **192**(7–8), 803–829.

Reddy, B. D. (1998) *Introductory Functional Analysis with Applications to Boundary Value Problems and Finite Elements*. Springer, New York.

Sokolowski, J. and Zochowski, A. (1999) On the topological derivative in shape optimization. *SIAM Journal on Control and Optimization*, **37**(4), 1251–1272.

Sokolowski, J. and Zolésio, J.-P. (1992) *Introduction to Shape Optimization: Shape Sensitivity Analysis*. Springer, Berlin.

Stein, E. (2003) *Error-controlled Adaptive Finite Elements in Solid Mechanics*. Wiley, Chichester.

Verfürth, R. (1996) *A Review of a Posteriori Error Estimation and Adaptive Mesh Refinement Techniques*. Wiley-Teubner, Chichester.

Zienkiewicz, O. C. and Craig, A. (1986) Adaptive refinement, error estimates, multigrid solution, and hierarchic finite element method concepts. In: I. Babuška, O. C. Zienkiewicz, J. Gago, and E. Oliviera, eds., *Accuracy Estimates and Adaptive Refinements in Finite Element Computations*, John Wiley & Sons, New York, 25–59.

Zienkiewicz, O. C., Gago, J., and Kelly, D. W. (1983) The hierarchical concept in finite element analysis. *Computers and Structures*, **16**(1–4), 53–65.